INTERNATIONAL JOURNAL FOR NUMERICAL METHODS IN FLUIDS, VOL. 25, 205–227 (1997)

NUMERICAL SOLUTIONS OF OPTIMAL CONTROL FOR THERMALLY CONVECTIVE FLOWS

S. S. RAVINDRAN*

Center for Research in Scientific Computation, Department of Mathematics, North Carolina State University, Raleigh, NC 27695-8205, U.S.A.

SUMMARY

We study the numerical solution of optimal control problems associated with two-dimensional viscous incompressible thermally convective flows. Although the techniques apply to more general settings, the presentation is confined to the objectives of minimizing the vorticity in the steady state case and tracking the velocity field in the non-stationary case with boundary temperature controls. In the steady state case we develop a systematic way to use the Lagrange multiplier rules to derive an optimality system of equations from which an optimal solution can be computed; finite element methods are used to find approximate solutions for the optimality system of equations. In the time-dependent case a piecewise-in-time optimal control approach is proposed and the fully discrete approximation algorithm for solving the piecewise optimal control problem is defined. Numerical results are presented for both the steady state and time-dependent optimal control problems.

Int. J. Numer. Meth. Fluids, **25**: 205–223, 1997.

No. of Figures: 2. No. of Tables: 0. No. of References: 9.

KEY WORDS: optimal control; Navier–Stokes equations; finite element method

1. INTRODUCTION

In past years, control of fluid flows has received considerable attention owing to its applicability in flow separation, combustion, fluid–structure interaction, design of novel submarine propulsion devices and modelling of nuclear reactors. It has been demonstrated in various experiments that control mechanisms such as boundary velocity, boundary temperature, moving surfaces, application of electromagnetic force, etc. can provide effective tools for control of fluids.

This paper presents a systematic study on numerical approximation and simulation of control of fluid flows using boundary temperature as control mechanism. In order to keep the illustration of ideas and computation easy, we restrict our study to cavity and expanding channel domains and the fluid is assumed to be incompressible.

The control objective in the context of optimal control problems is usually stated as the minimization of a cost functional such as the vorticity functional

$$\mathscr{J}(\mathbf{u}) = \int_{\Omega^*} |\nabla \times \mathbf{u}|^2 \mathrm{d}\Omega$$

* Correspondence to: S. S. Ravindran, Center for Research in Scientific Computation, Department of Mathematics, North Carolina State University, Raleigh, NC 27695-8205, U.S.A.

Contract grant sponsor: Air Force Office of Scientific Research; Contract grant number: AFOSR F49620-95-1-0437;
Contract grant number: AFOSR F49620-95-1-0447

CCC 0271–2091/97/020205–19 $17.50 *Received 15 April 1996*

Revised 4 October 1996

or the velocity-tracking functional

$$\mathscr{J}(\mathbf{u}) = \int_{\Omega^*} |\mathbf{u} - \mathbf{U}|^2 \mathrm{d}\Omega,$$

where $\mathbf{U}$ is a desired velocity, Ω^* is a part or the whole of the flow domain Ω and the flow is assumed stationary. The controls are some physical parameters that can be adjusted in practice, such as the velocity or temperature at the boundary.

We cast the control problem as a constrained minimization problem with appropriate costs and constraints depending on the problem under investigation. Our next step towards numerical resolution of the control problem is to derive relevant necessary conditions of optimality characterizing the control. Once we have the necessary conditions of optimality, we approximate them with finite elements and employ Newton's method to solve the finite-dimensional form of the necessary conditions of optimality. For high-Reynolds-number flows we employ Reynolds number marching to carry out the computations.

1.1. Description of steady state optimal control problem

In the steady state case we study vorticity minimization in channel flows as a prototype problem to illustrate our methods and results. It has been seen in channel flows with sudden expansion that near the corner region a recirculation appears, the size of which increases with increasing Reynolds number. Figure 1(a) (see Section 2.3) qualitatively illustrates the flow situation for high Reynolds numbers. Our objective is to suppress this recirculation by adjusting the temperature on a part of the boundary of the channel. Therefore we consider the following control problem. Find a candidate velocity–pressure–temperature triple ($\mathbf{u}$, p, T) by appropriately controlling (adjusting) the boundary temperature g such that the vorticity $\boldsymbol{\omega} = \nabla \times \mathbf{u}$ in the corner region Ω^* (see Figure 1(h)) of the channel is minimized. Precisely, we will study the following optimal control problem. Find ($\mathbf{u}$, p, T, g) such that the functional

$$\mathscr{J}(\mathbf{u}, g) = \frac{1}{2}\int_{\Omega^*} |\nabla \times \mathbf{u}|^2 \mathrm{d}\Omega + \frac{\beta}{2}\int_{\Gamma_{\mathrm{tb}}} |g|^2 \mathrm{d}\Gamma \tag{1}$$

is minimized subject to

$$-\frac{1}{Re}\Delta\mathbf{u} + (\mathbf{u}\cdot\nabla)\mathbf{u} + \nabla p + \frac{lg_0}{u_0^2} T\mathbf{g} = \mathbf{f} \quad \text{in } \Omega, \tag{2}$$

$$\nabla \cdot \mathbf{u} = 0 \quad \text{in } \Omega, \tag{3}$$

$$-\frac{\gamma}{RePr}\Delta T + \mathbf{u}\cdot\nabla T = 0 \quad \text{in } \Omega, \tag{4}$$

with the boundary conditions as follows. Let $\Gamma = \Gamma_{\mathrm{in}} \cup \Gamma_{\mathrm{out}} \cup \Gamma_{\mathrm{s}} \cup \Gamma_{\mathrm{tb}}$ be the boundary of our domain Ω. Then

$$\mathbf{u} = \mathbf{u}_{\mathrm{in}} \quad \text{and} \quad \frac{\partial T}{\partial n} = 0 \quad \text{on } \Gamma_{\mathrm{in}},$$

$$\mathbf{u} = \mathbf{u}_{\mathrm{out}} \quad \text{and} \quad \frac{\partial T}{\partial n} = 0 \quad \text{on } \Gamma_{\mathrm{out}},$$

$$\mathbf{u} = \mathbf{0} \quad \text{and} \quad \frac{\partial T}{\partial \mathbf{n}} = h(g(\mathbf{x}) - T) \quad \text{on} \quad \Gamma_{\mathrm{tb}} = \Gamma_{\mathrm{top}} \cup \Gamma_{\mathrm{bottom}},$$

$$\mathbf{u} = \mathbf{0} \quad \text{and} \quad T = T_1(\mathbf{x}) \quad \text{on } \Gamma_{\mathrm{s}},$$

where $\mathbf{u}_0$, T_0 and T_1 are given functions on the boundary, $\mathbf{g}$ is the gravity vector and g is the temperature control by radiational heating or cooling. In the cost functional $\mathscr{J}$ the term $\int_{\Omega^*} |\nabla \times \mathbf{u}|^2 \mathrm{d}\Omega$ is the vorticity in the L^2-norm, which measures the turbulence in the flow, the term $\int_\Gamma |g|^2 \mathrm{d}\Gamma$ is the measure of the magnitude of the control applied on the boundary, which is also required for the rigorous mathematical analysis of the control problem, and the penalizing parameter β adjusts the size of the terms in the cost. The flow quantities $\mathbf{u}$, T and p denote as usual the velocity, temperature and pressure respectively. The parameters Re, Pr and γ are the Reynolds number, Prandtl number and specific heat ratio respectively and l, g_0 and u_0 are the characteristic length, gravity and velocity respectively. A derivation of the system (2)–(4), known in the literature as the Boussinesq model, is given in Reference 1.

1.2. Description of time-dependent optimal control problem

In the time-dependent case we will use a velocity-tracking problem to illustrate our ideas and methods. We look for a candidate velocity–pressure–temperature triplet ($\mathbf{u}$, p, T) by controlling the boundary temperature g piecewise in time such that $\mathbf{u}$ 'best matches' a target velocity field $\mathbf{U}$. We try to match the velocity fields at a sequence of time intervals; the velocity tracking at each time interval is formulated as an optimal control problem. Precisely, we will study the following piecewise (in time) optimal control problem.

1. First, choose a sufficiently small $\delta > 0$, choose a sequence $\{t_n\}_{n=0}^N$ defined by $t_n = n\delta$ and define $\mathbf{u}^{(0)} = \mathbf{u}_0$ and $T^{(0)} = T_0$.
2. Then, inductively, for each n find a solution $(\mathbf{u}^{(n)}, p^{(n)}, T^{(n)}, g^{(n)})$ on the interval (t_{n-1}, t_n) which minimizes the instantaneous cost functional

$$\mathscr{J}_{t_n}(\mathbf{u}(t_n, \cdot), g(t_n, \cdot)) = \frac{1}{2}\int_\Omega |\mathbf{u}(t_n, \cdot) - \mathbf{U}|^2 \mathrm{d}\Omega + \frac{\beta}{2}\int_\Gamma |g(t_n, \cdot)|^2 \mathrm{d}\Gamma$$

subject to the two-dimensional state equations

$$\partial_t \mathbf{u}(t_n, \cdot) - \frac{1}{Re}\Delta \mathbf{u}(t_n, \cdot) + (\mathbf{u}(t_n, \cdot) \cdot \nabla)\mathbf{u}(t_n, \cdot) + \nabla p(t_n, \cdot) + \frac{lg_0}{u_0^2} T(t_n, \cdot)\mathbf{g} = \mathbf{f} \quad \text{in } \Omega, \tag{5}$$

$$\nabla \cdot \mathbf{u}(t_n, \cdot) = 0 \quad \text{in } \Omega, \tag{6}$$

$$\partial_t T(t_n, \cdot) - \frac{\gamma}{RePr}\Delta T(t_n, \cdot) + \mathbf{u}(t_n, \cdot) \cdot \nabla T(t_n, \cdot) = 0 \quad \text{in } \Omega, \tag{7}$$

with the boundary conditions

$$\mathbf{u}(t_n, \cdot) = \mathbf{0} \quad \text{and} \quad \frac{\partial T(t_n, \cdot)}{\partial \mathbf{n}} = h(g(t_n, \cdot) - T(t_n, \cdot)) \quad \text{on } \Gamma,$$

$$\mathbf{u}(t_{n-1}, \cdot) = \mathbf{u}^{(n-1)}(t_{n-1}) \quad \text{and} \quad T(t_{n-1}, \cdot) = T^{(n-1)}(t_{n-1}) \quad \text{in } \Omega.$$

We define a global (in time) solution ($\mathbf{u}$, p, T, g) by patching together all the local optimal control solutions $(\mathbf{u}^{(n)}, p^{(n)}, T^{(n)}, g^{(n)})$.

We will propose an algorithm for solving this problem with finite element discretization in space and first-order finite difference discretization in time.

It should be noted that the piecewise-in-time optimal control problem is different from the global optimal control problem defined as follows. Seek a $(\mathbf{u}, p, T, g)$ such that the functional

$$\mathscr{J}_{(0,T)}(\mathbf{u}, g) = \frac{1}{2}\int_0^T \int_\Omega |\mathbf{u} - \mathbf{U}|^2 \mathrm{d}\Omega \mathrm{d}t + \frac{\beta}{2}\int_0^T \int_\Omega |g|^2 \mathrm{d}\Gamma \mathrm{d}t$$

is minimized subject to the two-dimensional state equations

$$\partial_t \mathbf{u} - \frac{1}{Re}\Delta \mathbf{u} + (\mathbf{u} \cdot \nabla)\mathbf{u} + \nabla p + \frac{lg_0}{u_0^2} T\mathbf{g} = \mathbf{f} \quad \text{in } \Omega \times (0, T),$$

$$\nabla \cdot \mathbf{u} = 0 \quad \text{in } \Omega \times (0, T),$$

$$\partial_t T - \frac{\gamma}{RePr}\Delta T + \mathbf{u} \cdot \nabla T = 0 \quad \text{in } \Omega \times (0, T),$$

with the boundary conditions

$$\mathbf{u} = \mathbf{0} \quad \text{and} \quad \frac{\partial T}{\partial \mathbf{n}} = h(g(\mathbf{x}) - T) \quad \text{on } \Gamma \times (0, T),$$

$$\mathbf{u}(\cdot, 0) = \mathbf{u}_0 \quad \text{and} \quad T(\cdot, 0) = T_0 \quad \text{in } \Omega.$$

The piecewise-in-time optimal control problem can be thought of as the minimization of $\mathbf{u} - \mathbf{U}$ and g in some L^∞-norm, whereas the global optimal control problem is the minimization of these quantities in the $L^2(0, T)$-norm. We would like to point out here that the control obtained from the piecewise-in-time optimal control problem is *suboptimal* and there is no guarantee that it will be the same as that obtained from the global-in-time optimal control problem. However, as will be seen later, the piecewise optimal control approach does a very good job in tracking the velocity field. The piecewise-in-time optimal control problem can be solved by marching in time and thus requires essentially the same computer storage as the steady state optimal control problem. In contrast, the numerical solution of the global optimal control problem involves a time-dependent optimality system of equations with both initial and terminal conditions. Such a time-dependent optimality system has to be solved either with full time–space storage or by some iterative scheme that uncouples the initial and terminal conditions. In any case, it seems that in the context of flow matching and some other situations the numerical solution of the piecewise optimal control problem is more straightforward and efficient than that of the global optimal control problem.

2. FINITE ELEMENT SOLUTION OF STEADY STATE OPTIMAL CONTROL PROBLEM

In this section we develop a finite element algorithm for solving the steady state optimal control problem described in Section 1.1. We will first formally derive an optimality system of equations from which the optimal solutions can be computed. Then we define a finite element algorithm for solving this optimality system of equations. At the end of this section we present a numerical example.

2.1. An optimality system of equations

To facilitate the derivation of an optimality system and the approximation by finite elements, we rewrite the governing flow equations in a variational form. To this end we first introduce some

function spaces. We denote by $L^2(\Omega)$ the collection of square-integrable functions defined on Ω and we denote the associated norm by $\|\cdot\|_0$. Let

$$H^1(\Omega) = \left\{ v \in L^2(\Omega) \colon \frac{\partial v}{\partial x_i} \in L^2(\Omega) \quad \text{for} \quad i = 1, 2 \right\},$$

$$H_0^1(\Omega) = \{ v \in H^1 \colon \ v|_\Gamma = 0 \},$$

$$L_0^2(\Omega) = \left\{ q \in L^2(\Omega) \colon \int_\Omega q \mathrm{d}\Omega = 0 \right\},$$

$$H^m(\Omega) = \left\{ v \in L^2(\Omega) \colon \frac{\partial^{|\alpha|} v}{\partial x_1^{\alpha_1} \partial x_2^{\alpha_2}} \in L^2(\Omega) \quad \text{for all } \alpha = (\alpha_1, \alpha_2) \quad \text{with} \quad |\alpha| \leqslant m \right\}$$

and we denote the norm on $H^m(\Omega)$ by $\|\cdot\|_m$. Vector-valued counterparts of these spaces are denoted by boldface symbols, e.g. $\mathbf{H}^1 = [H^1]^2$.

We further define $\mathbf{H}_\mathbf{b}^1(\Omega) = \{ \mathbf{u} \in \mathbf{H}^1(\Omega) \colon \ \mathbf{u}|_\Gamma = \mathbf{b} \}$, $Z(\Omega) = \{ T \in H^1(\Omega) \colon \ T|_{\Gamma_s} = T_1 \}$ and $Z_0(\Omega) = \{ T \in H^1(\Omega) \colon \ T|_{\Gamma_s} = 0 \}$.

The conservative variational formulation of the steady state equations is then defined as follows. Seek $(\mathbf{u}, p, T) \in \mathbf{H}^1(\Omega) \times L_0^2(\Omega) \times H^1(\Omega)$ with $\mathbf{u}|_\Gamma = \mathbf{b}$ and $T|_{\Gamma_s} = T_1$ such that

$$\nu \int_\Omega \nabla \mathbf{u} : \nabla \mathbf{v} \mathrm{d}\Omega + \frac{1}{2} \int_\Omega [(\mathbf{u} \cdot \nabla)\mathbf{u} \cdot \mathbf{v} - (\mathbf{u} \cdot \nabla)\mathbf{v} \cdot \mathbf{u}] \mathrm{d}\Omega - \int_\Omega p \nabla \cdot \mathbf{v} \mathrm{d}\Omega + \alpha \int_\Omega T \mathbf{g} \cdot \mathbf{v} \mathrm{d}\Omega$$

$$= \int_\Omega \mathbf{f} \cdot \mathbf{v} \mathrm{d}\Omega \quad \forall \mathbf{v} \in \mathbf{H}_0^1(\Omega), \tag{8}$$

$$- \int_\Omega q \nabla \cdot \mathbf{u} \mathrm{d}\Omega = 0 \quad \forall q \in L_0^2(\Omega), \tag{9}$$

$$\kappa \int_\Omega \nabla T \cdot \nabla \psi \mathrm{d}\Omega + \frac{1}{2} \int_\Omega (\mathbf{u} \cdot \nabla T \psi - \mathbf{u} \cdot \nabla \psi T) \mathrm{d}\Omega + \kappa h \int_{\Gamma_{tb}} (T - g) \psi \mathrm{d}\Gamma = 0 \quad \forall \psi \in Z_0(\Omega). \tag{10}$$

Here the colon notation stands for the scalar product on $\mathbb{R}^{2 \times 2}$, $\alpha = l g_0 / u_0^2$, $\kappa = \gamma / RePr$ and $\mathbf{b}$ is the boundary prescription of velocity as elaborated in Section 1.1.

Remark

We note here that we have used antisymmetrized trilinear forms such as $\frac{1}{2}[\int_\Gamma (\mathbf{u} \cdot \nabla)\mathbf{v} \cdot \mathbf{w} \mathrm{d}\Omega - \int_\Omega (\mathbf{u} \cdot \nabla)\mathbf{w} \cdot \mathbf{v} \mathrm{d}\Omega]$ in place of $\int_\Omega (\mathbf{u} \cdot \nabla)\mathbf{w} \cdot \mathbf{v} \mathrm{d}\Omega$ in our variational formulation. The variational form defined in this way allows us to define consistent, stable and convergent finite element approximations of the state and of the optimality system to be defined in later sections. This type of variational form was introduced in Reference 2 for the purpose of proving the above-mentioned three properties of the finite element approximation of the Navier– Stokes equations. However, our computational experience is that the conservative formulation must be used in computations as well to avoid having non-physical solutions.

The steady state optimal control problem we wish to solve can now be stated as follows. *Seek a* $(\mathbf{u}, p, T, g) \in \mathbf{H}^1(\Omega) \times L_0^2(\Omega) \times H^1(\Omega) \times L^2(\Gamma_{tb})$ *with* $\mathbf{u}|_\Gamma = \mathbf{b}$ *and* $T|_{\Gamma_s} = T_1$ *such that the functional (1) is minimized subject to the constraints (8)–(10).*

Using Lagrange multiplier principles, we may turn this constrained optimization problem into an unconstrained one. Rigorous justification of the existence of optimal solutions and the derivation of necessary conditions of optimality for optimal control of fluid flows are given in e.g. References 3–6.

To make the abstract theories in optimal control more amenable to the derivation of an optimality system of equations, we introduce the following formal procedure. We set $X = \mathbf{H}_{\mathbf{b}}^1(\Omega) \times L_0^2(\Omega) \times Z(\Omega) \times \mathbf{H}_0^1(\Omega) \times L_0^2(\Omega) \times Z_0(\Omega) \times L^2(\Gamma_{\text{tb}})$ and define the Lagrangian functional

$$\begin{aligned}\mathscr{L}(\mathbf{u}, p, T, \boldsymbol{\mu}, \pi, \zeta, g) = \mathscr{J}(\mathbf{u}, g) - \nu \int_\Omega \nabla \mathbf{u} : \nabla \boldsymbol{\mu} \mathrm{d}\Omega - \frac{1}{2}\int_\Omega [(\mathbf{u} \cdot \nabla)\mathbf{u} \cdot \boldsymbol{\mu} - (\mathbf{u} \cdot \nabla)\boldsymbol{\mu} \cdot \mathbf{u}]\mathrm{d}\Omega \\ + \int_\Omega p \nabla \cdot \boldsymbol{\mu} \mathrm{d}\Omega + \int_\Omega \mathbf{f} \cdot \boldsymbol{\mu} \mathrm{d}\Omega - \alpha \int_\Omega T\mathbf{g} \cdot \boldsymbol{\mu} \mathrm{d}\Omega + \int_\Omega \pi \nabla \cdot \mathbf{u} \mathrm{d}\Omega \\ - \kappa \int_\Omega \nabla T \cdot \nabla \zeta \mathrm{d}\Omega - \frac{1}{2}\int_\Omega (\mathbf{u} \cdot \nabla T\zeta - \mathbf{u} \cdot \nabla \zeta T)\mathrm{d}\Omega \\ - \kappa h \int_{\Gamma_{\text{tb}}} (T - g)\zeta \mathrm{d}\Gamma \quad \forall (\mathbf{u}, p, T, \boldsymbol{\mu}, \pi, \zeta, g) \in X.\end{aligned}$$

Note that the Lagrangian is obtained by subtracting from the cost functional the variational form of the Navier–Stokes equations tested against the multipliers ($\boldsymbol{\mu}$, π, ζ) (which are also termed the adjoint state variables). An optimality system of equations that an optimum must satisfy is derived by taking variations with respect to each variable in the Lagrangian. By taking variations with respect to $\boldsymbol{\mu}$, ζ and π, we simply recover the constraint equations (8)–(10). By taking variation with respect to g, we obtain

$$\int_{\Gamma_{\text{tb}}} (\beta g + \kappa h \zeta) z \mathrm{d}\Gamma = 0 \quad \forall z \in L^2(\Gamma_{\text{tb}}), \quad \text{i.e.} \quad g = \frac{-\kappa h}{\beta}\zeta.$$

This last equation enables us to eliminate the control g in (10) to obtain

$$\begin{aligned}\nu \int_\Omega \nabla \mathbf{u} : \nabla \mathbf{v} \mathrm{d}\Omega + \frac{1}{2}\int_\Omega [(\mathbf{u} \cdot \nabla)\mathbf{u} \cdot \mathbf{v} - (\mathbf{u} \cdot \nabla)\mathbf{v} \cdot \mathbf{u}]\mathrm{d}\Omega - \int_\Omega p \nabla \cdot \mathbf{v} \mathrm{d}\Omega \\ + \alpha \int_\Omega T\mathbf{g} \cdot \mathbf{v} \mathrm{d}\Omega = \int_\Omega \mathbf{f} \cdot \mathbf{v} \mathrm{d}\Omega \quad \forall \mathbf{v} \in \mathbf{H}_0^1(\Omega), \end{aligned} \tag{11}$$

$$\int_\Omega q \nabla \cdot \mathbf{u} \mathrm{d}\Omega = 0 \quad \forall q \in L_0^2(\Omega), \tag{12}$$

$$\kappa \int_\Omega \nabla T \cdot \nabla \psi \mathrm{d}\Omega + \frac{1}{2}\int_\Omega (\mathbf{u} \cdot \nabla T\psi - \mathbf{u} \cdot \nabla \psi T)\mathrm{d}\Omega + \kappa h \int_{\Gamma_{\text{tb}}} \left(T + \frac{\kappa h}{\beta}\zeta\right)\psi \mathrm{d}\Gamma = 0 \quad \forall \psi \in Z_0(\Omega). \tag{13}$$

By taking variations with respect to $\mathbf{u}$, T and p, we obtain

$$\begin{aligned}\nu \int_\Omega \boldsymbol{\mu} : \nabla \mathbf{w} \mathrm{d}\Omega + \frac{1}{2}\int_\Omega [(\mathbf{u} \cdot \nabla)\mathbf{w} \cdot \boldsymbol{\mu} - (\mathbf{u} \cdot \nabla)\boldsymbol{\mu} \cdot \mathbf{w} + (\mathbf{w} \cdot \nabla)\mathbf{u} \cdot \boldsymbol{\mu} - (\mathbf{w} \cdot \nabla)\mathbf{u} \cdot \boldsymbol{\mu}]\mathrm{d}\Omega - \int_\Omega \pi \nabla \cdot \mathbf{w} \mathrm{d}\Omega \\ + \frac{1}{2}\int_\Omega (\mathbf{v} \cdot \nabla T\zeta - \mathbf{v} \cdot \nabla \zeta T)\mathrm{d}\Omega = \int_{\Omega^*} \nabla \times \mathbf{u} \cdot \nabla \times \mathbf{w} \mathrm{d}\Omega \quad \forall \mathbf{w} \in \mathbf{H}_0^1(\Omega), \end{aligned} \tag{14}$$

$$\int_\Omega \sigma \nabla \cdot \boldsymbol{\mu} \mathrm{d}\Omega = 0 \quad \forall \sigma \in L_0^2(\Omega), \tag{15}$$

$$\kappa \int_\Omega \nabla \zeta \cdot \nabla \psi \mathrm{d}\Omega + \frac{1}{2}\int_\Omega (\mathbf{u} \cdot \nabla \psi\zeta - \mathbf{u} \cdot \nabla \zeta\psi)\mathrm{d}\Omega + \alpha \int_\Omega \boldsymbol{\mu} \cdot \mathbf{g}\psi \mathrm{d}\Omega + \kappa h \int_{\Gamma_{\text{tb}}} \zeta\psi \mathrm{d}\Gamma = 0 \quad \forall \psi \in Z_0(\Omega). \tag{16}$$

Equations (11)–(16) together with $\mathbf{u}|_\Gamma = \mathbf{b}$ and $T|_{\Gamma_s} = T_1$ form an optimality system of equations that an optimal solution must satisfy. We will compute optimal solutions by solving this system of equations.

2.2. *Finite element approximations*

A finite element discretization of the optimality system consisting of (11)–(16), $\mathbf{u}|_\Gamma = \mathbf{b}$ and $T|_{\Gamma_s} = T_1$ is defined in the usual manner. First one chooses families of finite-dimensional subspaces $X_h \subset H^1(\Omega)$ and $S_h \subset L^2(\Omega)$. These families are parametrized by a parameter h that tends to zero; commonly, h is chosen to be some measure of the grid size. These finite-dimensional function spaces are defined on an approximate domain Ω_h. For simplicity we will state our results in this section by assuming $\Omega_h = \Omega$, which is the case when Ω is a convex polygon in two dimensions or a convex polyhedron in three dimensions. We assume that as $h \to 0$,

$$\inf_{\mathbf{v}_h \in \mathbf{X}_h} \int_\Omega [|\mathbf{v} - \mathbf{v}_h|^2 + |\nabla(\mathbf{v} - \mathbf{v}_h)|^2] \mathrm{d}\Omega \to 0 \quad \forall \mathbf{v} \in \mathbf{H}^1(\Omega),$$

$$\inf_{q_h \in S_h \cap L_0^2(\Omega)} \int_\Omega |q - q_h|^2 \mathrm{d}\Omega \to 0 \quad \forall q \in L_0^2(\Omega).$$

Here we may choose any pair of subspaces X^h and S^h such that $\mathbf{X}^h \cap \mathbf{H}_0^1(\Omega)$ and $S^h \cap L_0^2(\Omega)$ can be used for finding finite element approximations of solutions of the Navier–Stokes equations with homogeneous Dirichlet conditions. Thus we make the following standard assumptions, which are exactly those employed in well-known finite element methods for the Navier–Stokes equations. First we have the approximation properties: there exists an integer k, independent of h, $\mathbf{v}$ and q, such that

$$\inf_{\mathbf{v}_h \in \mathbf{X}_h} \int_\Omega [|\mathbf{v} - \mathbf{v}_h|^2 + |\nabla(\mathbf{v} - \mathbf{v}_h)|^2] \mathrm{d}\Omega = O(h^{m+1}) \quad \forall \mathbf{v} \in \mathbf{H}^{m+1}(\Omega), \quad 1 \leqslant m \leqslant k,$$

$$\inf_{q_h \in S_h \cap L_0^2(\Omega)} \int_\Omega |q - q_h|^2 \mathrm{d}\Omega = O(h^m) \quad \forall q \in H^m(\Omega) \cap L_0^2(\Omega), \quad 1 \leqslant m \leqslant k.$$

Next we assume the *inf-sup condition* or *Ladyzhenskaya–Babuska–Brezzi condition*: there exists a constant C, independent of h, such that

$$\inf_{0 \neq q_h \in S_h \cap L_0^2(\Omega)} \sup_{\mathbf{0} \neq \mathbf{v}_h \in \mathbf{X}_h \cap \mathbf{H}_0^1(\Omega)} \frac{-\int_\Omega q_h \nabla \cdot \mathbf{v}_h \mathrm{d}\Omega}{\|\mathbf{v}_h\|_1 \|q_h\|_0} \geqslant C.$$

This condition assures the stability of finite element discretizations of the Navier–Stokes equations; see e.g. References 7 and 8. It also assures the stability of the approximation of the optimality system (11)–(16).[5] For thorough discussions of the approximation properties and the stability condition see e.g. References 7 and 8. References 7 and 8 may also be consulted for a catalogue of finite element subspaces that meet the requirements of the above approximation properties and the inf-sup condition.

Once the approximating subspaces have been chosen, we look for an approximate optimal solution $(\mathbf{u}_h, p_h, T_h, \boldsymbol{\mu}_h, \pi_h, \zeta_h) \in \mathbf{X}_h \times (S_h \cap L_0^2(\Omega)) \times X_h \times (\mathbf{X}_h \cap \mathbf{H}_0^1(\Omega)) \times (S_h \cap L_0^2(\Omega)) \times (X_h \cap Z_0)$ by solving the discrete optimality system of equations

$$\nu \int_\Omega \nabla \mathbf{u} : \nabla \mathbf{v}_h \mathrm{d}\Omega + \frac{1}{2}\int_\Omega [(\mathbf{u}_h \cdot \nabla)\mathbf{u}_h \cdot \mathbf{v}_h - (\mathbf{u}_h \cdot \nabla)\mathbf{v}_h \cdot \mathbf{u}_h]\mathrm{d}\Omega - \int_\Omega p_h \nabla \cdot \mathbf{v}_h \mathrm{d}\Omega + \alpha \int_\Omega T_h \mathbf{g} \cdot \mathbf{v}_h \mathrm{d}\Omega$$
$$= \int_\Omega \mathbf{f} \cdot \mathbf{v}_h \mathrm{d}\Omega \quad \forall \mathbf{v}_h \in \mathbf{X}_h \cap \mathbf{H}_0^1(\Omega), \tag{17}$$

$$\int_\Omega q_h \nabla \cdot \mathbf{u}_h \mathrm{d}\Omega = 0 \quad \forall q^h \in S_h \cap L_0^2(\Omega), \tag{18}$$

$$\kappa \int_\Omega \nabla T_h \cdot \nabla \psi_h \mathrm{d}\Omega + \frac{1}{2}\int_\Omega (\mathbf{u}_h \cdot \nabla T_h \psi_h - \mathbf{u}_h \cdot \nabla \psi_h T_h)\mathrm{d}\Omega + \kappa h \int_{\Gamma_{\mathrm{tb}}} \left(T_h + \frac{\kappa h}{\beta}\zeta_h\right)\psi_h \mathrm{d}\Gamma$$
$$= 0 \quad \forall \psi_h \in X_h \cap Z_0, \tag{19}$$

$$\nu \int_\Omega \nabla \boldsymbol{\mu}_h : \nabla \mathbf{w}_h \mathrm{d}\Omega + \frac{1}{2}\int_\Omega (\mathbf{v}_h \cdot \nabla) T_h \zeta_h - \mathbf{v}_h \cdot \nabla \zeta_h T_h)\mathrm{d}\Omega + \frac{1}{2}\int_\Omega [(\mathbf{u}_h \cdot \nabla)\mathbf{w}_h \cdot \boldsymbol{\mu}_h - (\mathbf{u}_h \cdot \nabla)\boldsymbol{\mu}_h \cdot \mathbf{w}_h]\mathrm{d}\Omega$$
$$+ \frac{1}{2}\int_\Omega [(\mathbf{w}_h \cdot \nabla)\mathbf{u}_h \cdot \boldsymbol{\mu}_h - (\mathbf{w}_h \cdot \nabla)\mathbf{u}_h \cdot \boldsymbol{\mu}_h]\mathrm{d}\Omega - \int_\Omega \pi_h \nabla \cdot \mathbf{w}_h \mathrm{d}\Omega$$
$$= \int_{\Omega^*} \nabla \times \mathbf{u}_h \cdot \nabla \times \mathbf{w}_h \mathrm{d}\Omega \quad \forall \mathbf{w}_h \in \mathbf{X}_h \cap \mathbf{H}_0^1(\Omega), \tag{20}$$

$$\int_\Omega r_h \nabla \cdot \boldsymbol{\mu}_h \mathrm{d}\Omega = 0 \quad \forall r^h \in S_h \cap L_0^2(\Omega), \tag{21}$$

$$\kappa \int_\Omega \nabla \zeta_h \cdot \nabla \psi_h \mathrm{d}\Omega + \frac{1}{2}\int_\Omega (\mathbf{u}_h \cdot \nabla \psi_h \zeta_h - \mathbf{u}_h \cdot \nabla \zeta_h \psi_h)\mathrm{d}\Omega + \alpha \int_\Omega \boldsymbol{\mu}_h \cdot \mathbf{g} \psi_h \mathrm{d}\Omega + \kappa h \int_{\Gamma_{\mathrm{tb}}} \zeta_h \psi_h \mathrm{d}\Gamma$$
$$= 0 \quad \forall \psi_h \in X_h \cap Z_0. \tag{22}$$

We point out that if a solution $(\mathbf{u}, p, T, \boldsymbol{\mu}, \pi, \zeta)$ for (11)–(16) with $\mathbf{u}|_\Gamma = \mathbf{b}$ and $T|_{\Gamma_s} = T_1$ belongs to $\mathbf{H}^{m+1}(\Omega) \times H^m(\Omega) \times \mathbf{H}^{m+1}(\Omega) \times \mathbf{H}^{m+1}(\Omega) \times H^m(\Omega) \times \mathbf{H}^{m+1}(\Omega)$, then we can find an approximate solution from (17)–(22) with the error estimate

$$\int_\Omega [|\mathbf{u} - \mathbf{u}_h|^2 + |\nabla(\mathbf{u} - \mathbf{u}_h)|^2 + |T - T_h|^2 + |\nabla(T - T_h)|^2 + |p - p_h|^2$$
$$+ |\boldsymbol{\mu} - \boldsymbol{\mu}_h|^2 + |\nabla(\boldsymbol{\mu} - \boldsymbol{\mu}_h)|^2 + |\zeta - \zeta_h|^2 + |\nabla(\zeta - \zeta_h)|^2 + |\pi - \pi_h|^2]\mathrm{d}\Omega \leqslant O(h^{m+1}).$$

We employ Newton's iteration method to solve the resulting non-linear algebraic system of equations for the nodal values of the unknowns, which can be written as

$$F_i(\mathscr{X}) = 0, \quad 1 \leqslant i \leqslant N,$$

where $\mathscr{X}$ is the vector of unknown nodal values and N is the number of unknowns. Then Newton's method is given as follows.

Algorithm 1

1. Triangulate the flow domain with a sufficiently small mesh size h; choose finite element spaces $\mathbf{X}_h$ and S_h; choose an initial guess $\mathscr{X}^{(0)}$.
2. For $n = 1, 2, \ldots$ compute $\mathscr{X}^{(n)}$ from the linear system

$$\frac{\partial F_i(\mathscr{X}^{(n-1)})}{\partial \mathscr{X}_j}(\mathscr{X}_j^{(n)} - \mathscr{X}_j^{(n-1)}) = -F_i(\mathscr{X}^{(n-1)}).$$

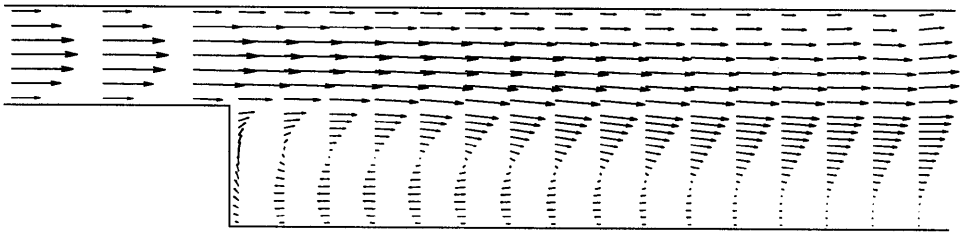

Figure 1(a). Stationary uncontrolled flow

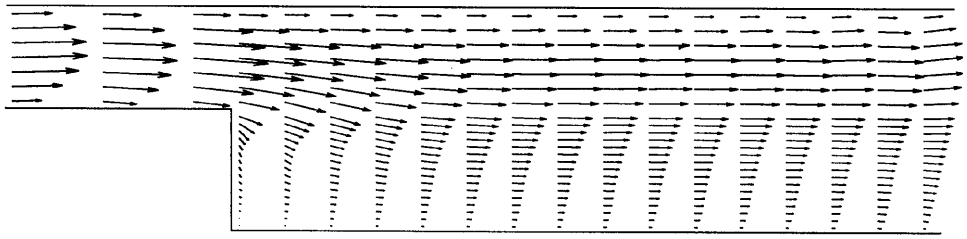

Figure 1(b). Stationary controlled flow

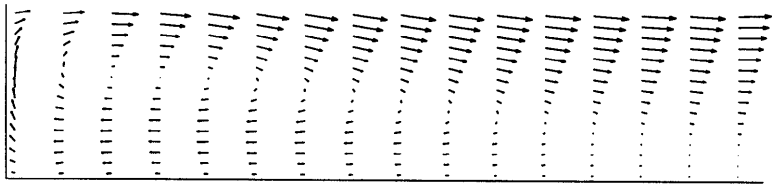

Figure 1(c). Partial enlargement of Figure 1(a)

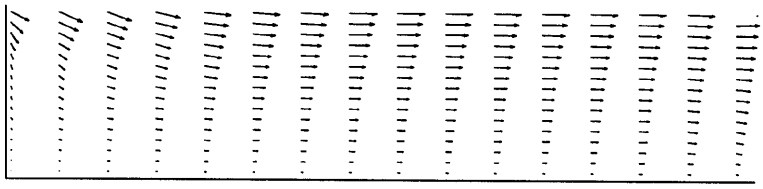

Figure 1(d). Partial enlargement of Figure 1(b)

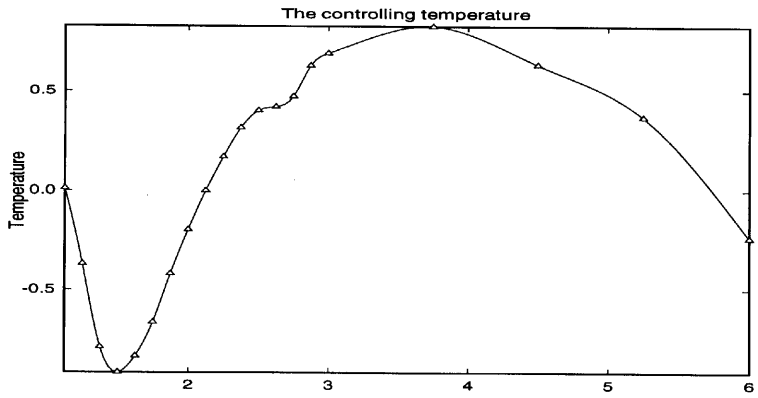

Figure 1(e). Control on boundary Γ_{bottom}

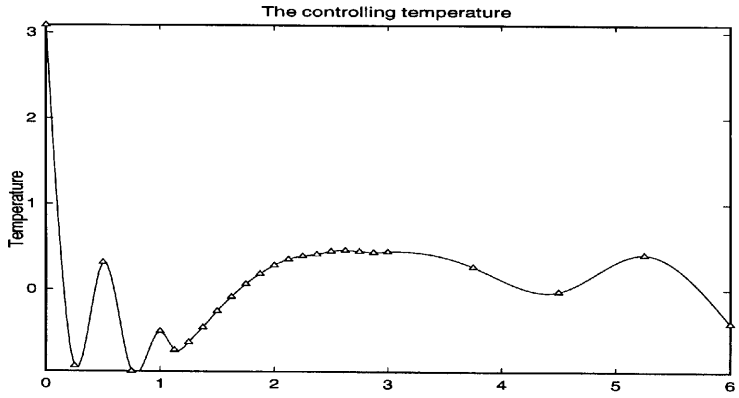

Figure 1(f). Control on boundary Γ_{top}

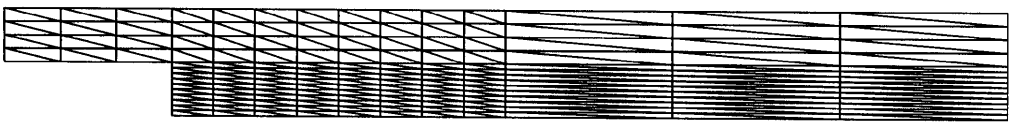

Figure 1(g). Triangulation of channel

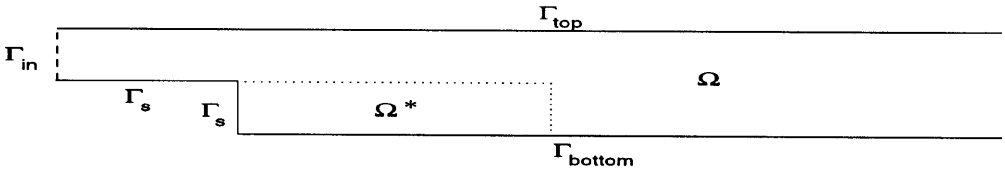

Figure 1(h). Channel with sudden expansion

At each Newton iteration we solve the linear system of equations by Gaussian elimination for banded matrices. Under suitable assumptions, Newton's method converges at a quadratic rate. Quadratic convergence of Newton's method is valid within a contraction ball. In order to obtain a good initial guess, we solve the the optimality system corresponding to the Stokes problem which is obtained by considering the minimization of the cost subject to the Stokes equations.

For high-Reynolds-number flows we employ Reynolds number marching, in which one considers a finite sequence of Reynolds numbers $R_1 < R_2 < \cdots < R_f$, with R_f being the desired Reynolds number, such that R_1 is small enough for Newton's method to converge with the proposed initial guess. Then the solution obtained with Reynolds number R_1 is used as initial guess for the computations with Reynolds number R_2. This process is continued until the desired Reynolds number is reached.

2.3. A vorticity minimization problem in channel flows

We consider the problem of minimizing the vorticity in a backward-facing step channel flow by maintaining a temperature gradient between the top and bottom channel walls. A schematic diagram of the channel geometry illustrating the part of the channel in which the vorticity is minimized is given in Figure 1(h).

As elaborated in Section 1.1, we minimize the functional (1) subject to (8)–(10). The optimality system of equations is given by (11)–(16) with $\mathbf{u}|_\Gamma = \mathbf{b}$ and $T|_{\Gamma_s} = T_1$.

The vorticity functional is minimized in the corner region of the channel $\Omega^* = (1, 3) \times (0, 0{\cdot}5)$; see Figure 1(h). The height of the inflow (left) boundary is 0·5 and that of the outflow (right) boundary is 1. The length of the narrower section of the channel is 1 and that of the wider section of the channel is 5 (the total horizontal length is 6). In the computation we choose the Reynolds number to be 200 ($\nu = 1/200$), the temperature $T_1 = 1$ on the step Γ_s of the channel boundary and the characteristic values for velocity, gravity and length are taken as $u_0 = 1$, $l = 0{\cdot}1$ and $g_0 = 9{\cdot}81$. We have chosen zero boundary condition for the velocity on the channel walls and non-zero boundary conditions

$$\mathbf{u} = \begin{pmatrix} 8(y - 0{\cdot}5)(1 - y) \\ 0 \end{pmatrix} \quad \text{at the inflow (right) boundary}$$

and

$$\mathbf{u} = \begin{pmatrix} (1 - y)y \\ 0 \end{pmatrix} \quad \text{at the outflow (right) boundary.}$$

The external body force $\mathbf{f}$ is chosen to be zero and the parameter in the functional is chosen as $\beta = 0{\cdot}01$.

The finite element space $\mathbf{X}_h$ is chosen to be piecewise quadratic elements (for $\mathbf{u}_h$, $\boldsymbol{\mu}_h$, T_h and ς_h) and S_h is chosen to be piecewise linear elements (for p_h and π_h). The computational domain is divided into 332 triangles, with a finer mesh around the corner of the step; see Figure 1(g). We use Algorithm 1 to find a finite element solution ($\mathbf{u}_h$, p_h, T_h, $\boldsymbol{\mu}_h$, π_h, ζ_h).

We obtain the optimal solution typically in seven Newton iterations starting with the Stokes solution as initial guess. At each Newton iteration a banded Gaussian elimination is used to solve the resulting linear system. Figure 1(b) gives the velocity field $\mathbf{u}_h$ of the optimal control solution. For comparison purposes we have also calculated the uncontrolled solution ($\mathbf{u}_0$, p_0, T_0) from (8)–(10) (with $g = 0$). The solution is given in Figure 1(a) (the velocity field on a section of the channel). Figures 1(c) and 1(d) are blow-ups of the uncontrolled and controlled flows respectively at the corner of the backward-facing step. The control distributions on the top and bottom walls are given in Figures 1(e) and 1(f). The values of the integral $\int_{\Omega^*} |\nabla \times \mathbf{u}|^2 d\Omega$ without and with controls are 1·07347

and 0·4778 respectively. We see that we achieved a reduction of 55·79 per cent in the $L^2(\Omega)$-norm of the vorticity. We would like to mention here that owing to the non-linearity in the state equations, the minimum we obtained may only be a local minimum and there is no reason to believe it is the global minimum.

By minimizing the functional (1), we wish to obtain a velocity distribution that has minimal vorticity. The numerical results, Figure 1(b) in particular, demonstrate that the optimal control did a very good job in achieving this objective.

3. FULLY DISCRETE APPROXIMATIONS OF TIME-DEPENDENT OPTIMAL CONTROL PROBLEM

In this section we first discretize the piecewise-in-time optimal control problem described in Section 1.2, we then propose an algorithm based on the discretizations and finally we report some numerical results.

3.1. Time and spatial discretizations of piecewise-in-time optimal control problem

In order to compute numerically the optimal solutions for the piecewise optimal control problem described in Section 1.2, we need to discretize this problem in both time and space.

We use the backward Euler scheme to approximate the derivatives $\partial_t \mathbf{u}$ and $\partial_t T$ and discretize the spatial variables by finite element methods. We choose families of finite element subspaces $\mathbf{X}_h \subset \mathbf{H}^1(\Omega)$ and $S_h \subset L^2(\Omega)$ as in Section 2.3. We also define $Y_h \subset L^2(\Gamma)$ for the approximate boundary controls. Once the finite element spaces $\boldsymbol{X}_h$ and S_h have been chosen, we define the fully discrete approximations of the piecewise optimal control problem as follows.

1. Set $\Delta t = \delta$.
2. Define $\mathbf{u}_h^0 = \mathbf{u}_{0,h}$ and $T_h^0 = T_{0,h}$, where $\mathbf{u}_{0,h}$ and $T_{0,h}$ are the $\mathbf{L}^2(\Omega)$-projection (or interpolation) of $\mathbf{u}_0$ and T_0 onto $\mathbf{X}_h \cap \mathbf{H}_0^1(\Omega)$ and X_h respectively.
3. *The $(n+1)$th fully discrete optimal control problem:* for $n = 0, 1, 2, \ldots$ find a $(\mathbf{u}_h^{n+1}, p_h^{n+1}, T_h^{n+1}, g_h^{n+1}) \in (\mathbf{X}_h \cap \mathbf{H}_0^1(\Omega)) \times X_h \times (S_h \cap L_0^2(\Omega)) \times Y_h$ such that the functional

$$\mathscr{J}_h^{n+1}(\mathbf{u}_h^{n+1}, g_h^{n+1}) = \frac{1}{2}\int_\Omega |\mathbf{u}_h^{n+1} - \mathbf{U}^{n+1}|^2 \mathrm{d}\Omega + \frac{\beta}{2}\int_\Gamma |g_h^{n+1}|^2 \mathrm{d}\Gamma$$

is minimized subject to the fully discrete state equations

$$\frac{1}{\Delta t}\int_\Omega \mathbf{u}_h^{n+1} \cdot \mathbf{w}_h \mathrm{d}\Omega + \nu \int_\Omega \nabla \mathbf{u}_h^{n+1} : \nabla \mathbf{w}_h \mathrm{d}\Omega - \int_\Omega p_h^{n+1} \nabla \cdot \mathbf{w}_h \mathrm{d}\Omega + \frac{1}{2}\int_\Omega [(\mathbf{u}_h^{n+1} \cdot \nabla)\mathbf{u}_h^{n+1} \cdot \mathbf{w}_h$$

$$- (\mathbf{u}_h^{n+1} \cdot \nabla)\mathbf{w}_h \cdot \mathbf{u}_h^{n+1}]\mathrm{d}\Omega = \int_\Omega \mathbf{f}_h^{n+1} \cdot \mathbf{w}_h \mathrm{d}\Omega + \frac{1}{\Delta t}\int_\Omega \mathbf{u}_h^n \cdot \mathbf{w}_h \mathrm{d}\Omega \quad \forall \mathbf{w}_h \in \mathbf{X}_h \cap \mathbf{H}_0^1(\Omega), \tag{23}$$

$$\int_\Omega r_h \nabla \cdot \mathbf{u}_h^{n+1} \mathrm{d}\Omega = 0 \quad \forall r_h \in S_h \cap L_0^2(\Omega), \tag{24}$$

$$\frac{1}{\Delta t}\int_\Omega T_h^{n+1}\psi_h \mathrm{d}\Omega + \kappa \int_\Omega \nabla T_h^{n+1} \cdot \nabla \psi_h \mathrm{d}\Omega + \frac{1}{2}\int_\Omega (\mathbf{u}_h^{n+1} \cdot \nabla T_h^{n+1}\psi_h - \mathbf{u}_h^{n+1} \cdot \nabla \psi_h T_h^{n+1})\mathrm{d}\Omega$$

$$+ \kappa h \int_\Gamma (T_h^{n+1} - g_h^{n+1})\psi_h \mathrm{d}\Gamma = \frac{1}{\Delta t}\int_\Omega T_h^n \psi_h \mathrm{d}\Omega \quad \forall \psi_h \in X_h. \tag{25}$$

3.2. An algorithm

In order to solve the $(n+1)$th fully discrete optimal control problem for each n, we need to introduce a Lagrange multiplier $(\boldsymbol{\mu}_h^{n+1}, \pi_h^{n+1}, \zeta_h^{n+1}) \in (\mathbf{X}_h \cap \mathbf{H}_0^1(\Omega)) \times (S_h \cap L_0^2(\Omega)) \times X_h$ to convert the $(n+1)$th fully discrete optimal control problem into a discrete optimality system of equations. A solution for the $(n+1)$th fully discrete optimal control problem can be found by solving the discrete optimality system of equations which consists of the fully discrete Navier–Stokes equations (given previously) and

$$\begin{aligned}
&\frac{1}{\Delta t}\int_\Omega \boldsymbol{\mu}_h^{n+1}\cdot\mathbf{w}_h\mathrm{d}\Omega + \nu\int_\Omega \nabla\boldsymbol{\mu}_h^{n+1} : \nabla\mathbf{w}_h\mathrm{d}\Omega - \int_\Omega \pi_h^{n+1}\nabla\cdot\mathbf{w}_h\mathrm{d}\Omega \\
&\quad + \frac{1}{2}\int_\Omega (\mathbf{v}_h\cdot\nabla T_h^{n+1}\zeta_h^{n+1} - \mathbf{v}_h\cdot\nabla\zeta_h^{n+1}T_h^{n+1})\mathrm{d}\Omega + \frac{1}{2}\int_\Omega [(\mathbf{u}_h^{n+1}\cdot\nabla)\mathbf{w}_h\cdot\boldsymbol{\mu}_h^{n+1} \\
&\quad - (\mathbf{u}_h^{n+1}\cdot\nabla)\boldsymbol{\mu}_h^{n+1}\cdot\mathbf{w}_h]\mathrm{d}\Omega \\
&\quad + \frac{1}{2}\int_\Omega [(\mathbf{w}_h\cdot\nabla)\mathbf{u}_h^{n+1}\cdot\boldsymbol{\mu}_h^{n+1} - (\mathbf{w}_h\cdot\nabla)\boldsymbol{\mu}_h^{n+1}\cdot\mathbf{u}_h^{n+1}]\mathrm{d}\Omega \\
&= \int_\Omega \nabla\times\mathbf{u}_h^{n+1}\cdot\nabla\times\mathbf{w}_h\mathrm{d}\Omega \quad \forall\mathbf{w}_h \in \mathbf{X}_h\cap\mathbf{H}_0^1(\Omega),
\end{aligned} \tag{26}$$

$$\int_\Omega r_h\nabla\cdot\boldsymbol{\mu}_h^{n+1}\mathrm{d}\Omega = 0 \quad \forall r^h \in S_h\cap L_0^2(\Omega), \tag{27}$$

$$\begin{aligned}
&\frac{1}{\Delta t}\int_\Omega \zeta_h^{n+1}\psi_h\mathrm{d}\Omega + \kappa\int_\Omega \nabla\zeta_h^{n+1}\cdot\nabla\psi_h\mathrm{d}\Omega + \alpha\int_\Omega \boldsymbol{\mu}_h^{n+1}\cdot\mathbf{g}\psi_h\mathrm{d}\Omega + \kappa h\int_\Gamma \zeta_h^{n+1}\psi_h\mathrm{d}\Gamma \\
&\quad + \frac{1}{2}\int_\Omega (\mathbf{u}_h^{n+1}\cdot\nabla\psi_h\zeta_h^{n+1} - \mathbf{u}_h^{n+1}\cdot\nabla\zeta_h^{n+1}\psi_h)\mathrm{d}\Omega = 0 \quad \forall\psi_h \in X_h
\end{aligned} \tag{28}$$

$$\int_\Gamma z_h g_h^{n+1} + \frac{\kappa h}{\beta} z_h\zeta_h^{n+1}\mathrm{d}\Gamma = 0 \quad \forall z_h \in Y_h. \tag{29}$$

Note that for each $n = 0, 1, 2, \ldots$ the $(n+1)$th optimal control problem is a *steady state* problem for the state variable triplet $(\mathbf{u}^{n+1}, p^{n+1}, T^{n+1})$ and the control variable g^{n+1}. We now summarize an algorithm for solving the fully discrete piecewise optimal control problem.

Algorithm 2

1. Choose a (sufficiently small) $\delta > 0$ and set $\Delta t = \delta$; choose a (sufficiently small) h along with the finite element spaces $\mathbf{X}_h$ and S_h.
2. Define $\mathbf{u}_h^0 = \mathbf{u}_{0,h}$ and $T_h^0 = T_{0,h}$, where $\mathbf{u}_{0,h}$ and $T_{0,h}$ are the $\mathbf{L}^2(\Omega)$-projection (or interpolation) of $\mathbf{u}_0$ and T_0 onto $\mathbf{X}_h\cap\mathbf{H}_0^1(\Omega)$ and X_h respectively.
3. For $n = 0, 1, 2, \ldots$ use Newton iterations to find a solution to (23)–(29).
4. Set $g_h^{n+1} = -\beta^{-1}\kappa h\zeta_h^{n+1}$ on Γ.

It should be noted that the numerical procedure for solving the system (23)–(29) is essentially the same as that for solving the optimality system in the steady state optimal control problem; see Section 2.2.

3.3. A velocity-tracking problem in cavity flows

We now report some computational results for solving the piecewise-in-time optimal control problem by implementing Algorithm 2. The example demonstrates that the piecewise optimal control does a very good job of tracking the velocity field. Also, in the solution process an optimal control distribution can be obtained. The test example in this section can be solved by a scheme which treats the advection term explicitly or by a Crank–Nicolson scheme, but for simplicity we will follow Algorithm 2 with a backward Euler implicit scheme.

Here are some detailed data of the example. We choose the domain $\Omega = (0, 1) \times (0, 1)$ (i.e. the unit square). The desired velocity field is taken to be four steady velocity fields in four different time intervals in [0, 1] as follows:

$$\mathbf{U}(\mathbf{x}) = \begin{pmatrix} [\cos(2\pi x) - 1]\sin(2\pi y) \\ -[\cos(2\pi y) - 1]\sin(2\pi x) \end{pmatrix} \quad \text{for} \quad 0 \leqslant t \leqslant 0{\cdot}25,$$

$$\mathbf{U}(\mathbf{x}) = \begin{pmatrix} \cos(2\pi y)[\cos(2\pi x) - 1] \\ \sin(2\pi x)\sin(2\pi y) \end{pmatrix} \quad \text{for} \quad 0{\cdot}25 < t \leqslant 0{\cdot}5,$$

$$\mathbf{U}(\mathbf{x}) = \begin{pmatrix} [\cos(2\pi x) - 1]\cos(2\pi y) \\ -[\cos(2\pi y) - 1]\cos(2\pi x) \end{pmatrix} \quad \text{for} \quad 0{\cdot}5 < t \leqslant 0{\cdot}75,$$

$$\mathbf{U}(\mathbf{x}) = \begin{pmatrix} \sin(2\pi x)\cos(2\pi y) \\ -\cos(2\pi x)\sin(2\pi y) \end{pmatrix} \quad \text{for} \quad 0{\cdot}75 < t \leqslant 1.$$

Note that $\mathbf{U}$ is defined in such a way that it satisfies the divergence- free condition. We choose the viscosity constant $v = 0{\cdot}1$, $h = 0{\cdot}1$ and the time step $\Delta t = \frac{1}{12}$ for the computation. All the other parameters and the finite element spaces to approximate the variables are taken to be the same as in the steady state problem.

The computational results obtained by implementing Algorithm 2 with the above data are presented in graphical form.

Figures 2(a)–(2f) show the controlled and desired flows in the first quarter of the time interval. Figures 2(a) and 2(b) show the initial states $\mathbf{U}_0$ and $\mathbf{u}_0$ of the desired and controlled flows. Note that $\mathbf{u}_0$ is far away from the zero vector field $\mathbf{U}_0$. During $0 \leqslant t \leqslant \frac{1}{12}$ the control is in the transient stage. Starting from $t = \frac{1}{12}$, the controlled flow matches the desired flow so well that they are hardly distinguishable by the naked eye (Figures 2(c)–2(f)) for $t = 0{\cdot}166$ and $0{\cdot}25$.

Figures 2(g)–2(l) show the controlled and desired flows in the second quarter of the time interval.

Figures 2(m)–2(r) show the controlled and desired flows in the third quarter of the time interval.

Figures 2(s)–2(x) show the controlled and desired flows in the fourth quarter of the time interval.

To summarize this example, we see that typically in the first time step of each quarter of the time interval the controlled velocity field is in a transient stage, but starting from the second step it is in nice agreement with the target field.

4. CONCLUSIONS

In this paper we studied two optimal control problems in thermally convective flows using boundary temperature controls: a vorticity minimization problem in steady channel flows and a velocity-tracking problem in unsteady cavity flows. We formulated each of the control problems as a constrained minimization problem with appropriate cost functional. The necessary conditions of

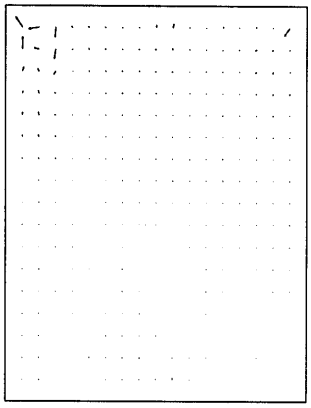

(a)

Figure 2(a). Controlled flow at $t = \frac{1}{12}$

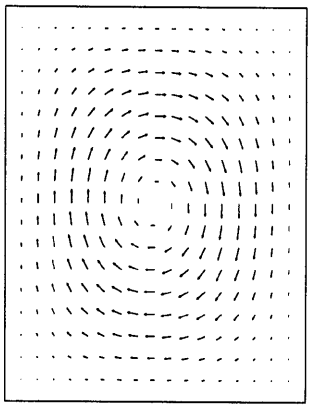

(b)

Figure 2(b). Desired flow at $t = \frac{1}{12}$

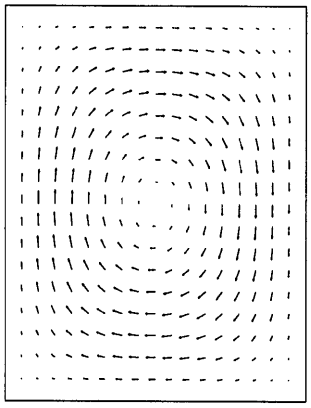

(c)

Figure 2(c). Controlled flow at $t = \frac{1}{6}$

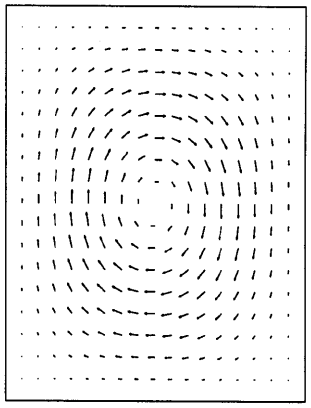

(d)

Figure 2(d). Desired flow at $t = \frac{1}{6}$

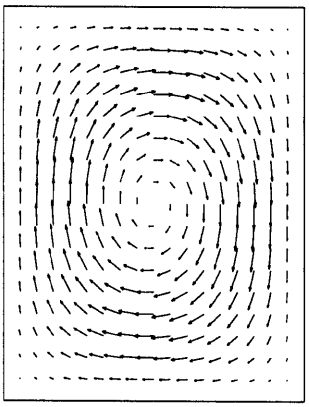

(e)

Figure 2(e). Controlled flow at $t = \frac{1}{4}$

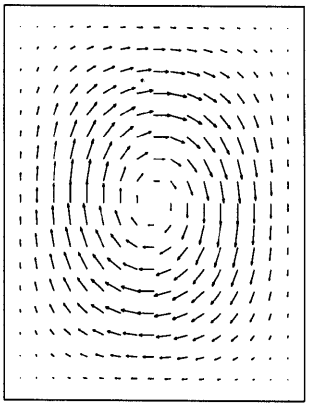

(f)

Figure 2(f). Desired flow at $t = \frac{1}{4}$

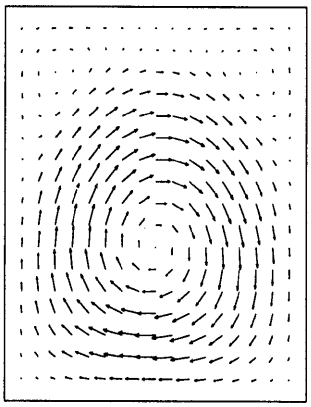

(g)

Figure 2(g). Controlled flow at $t = \frac{1}{3}$

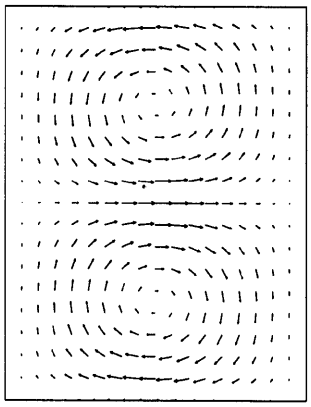

(h)

Figure 2(h). Desired flow at $t = \frac{1}{3}$

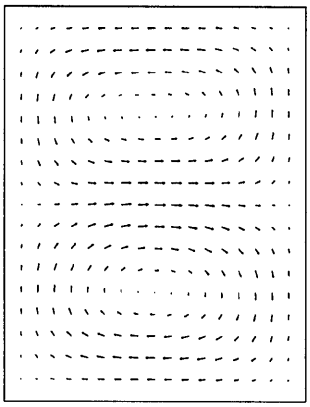

(i)

Figure 2(i). Controlled flow at $t = \frac{5}{12}$

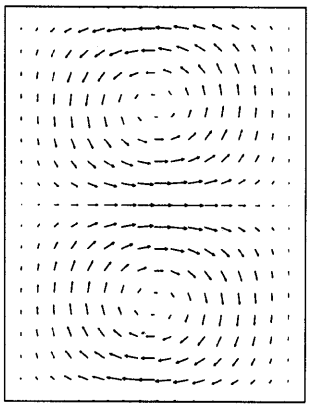

(j)

Figure 2(j). Desired flow at $t = \frac{5}{12}$

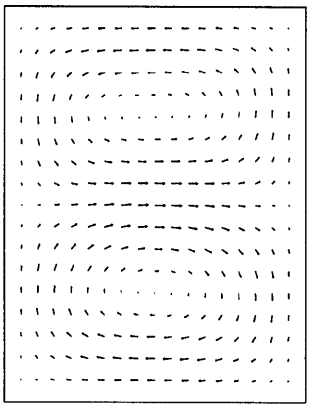

(i)

Figure 2(k). Controlled flow at $t = \frac{1}{2}$

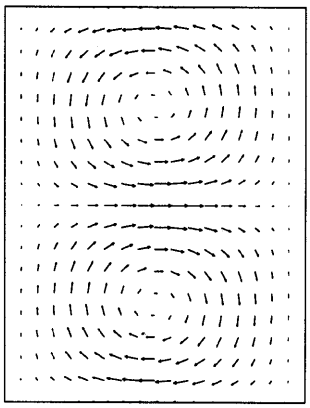

(j)

Figure 2(l). Desired flow at $t = \frac{1}{2}$

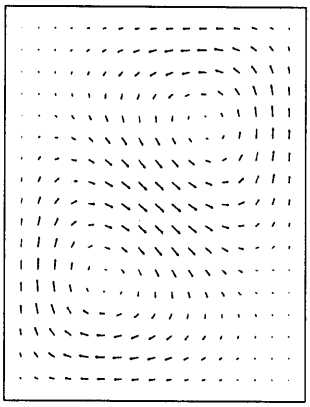

(m)

Figure 2(m). Controlled flow at $t = \frac{7}{12}$

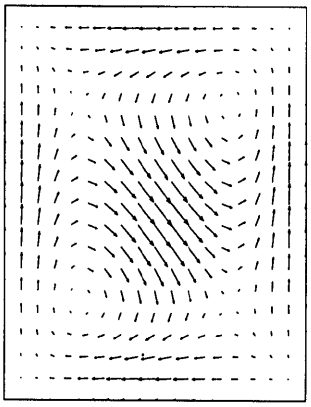

(n)

Figure 2(n). Desired flow at $t = \frac{7}{12}$

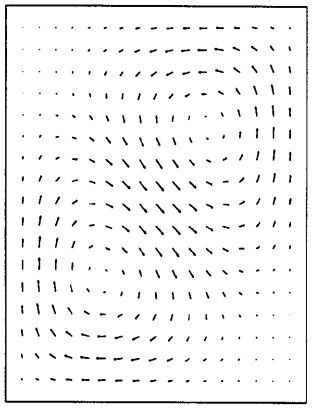

(o)

Figure 2(o). Controlled flow at $t = \frac{2}{3}$

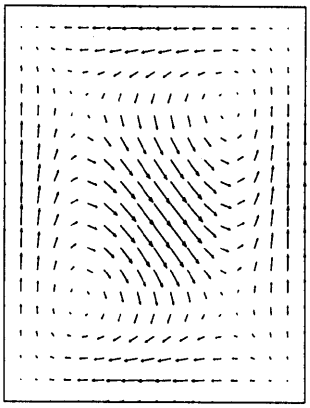

(p)

Figure 2(p). Desired flow at $t = \frac{2}{3}$

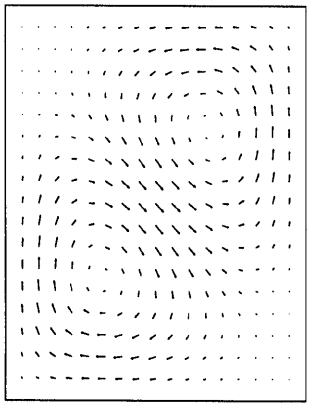

(q)

Figure 2(q). Controlled flow at $t = \frac{3}{4}$

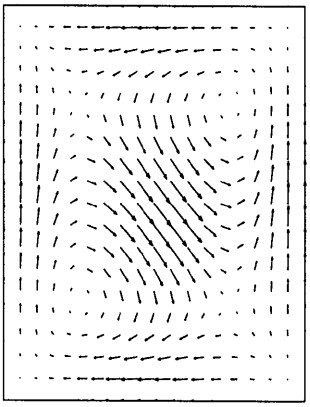

(r)

Figure 2(r). Desired flow at $t = \frac{3}{4}$

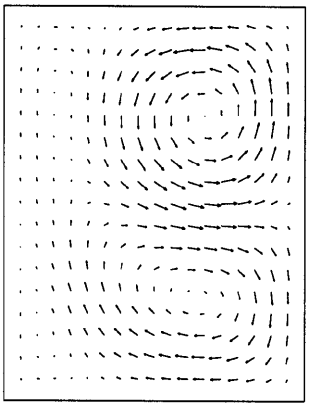

(s)

Figure 2(s). Controlled flow at $t = \frac{10}{12}$

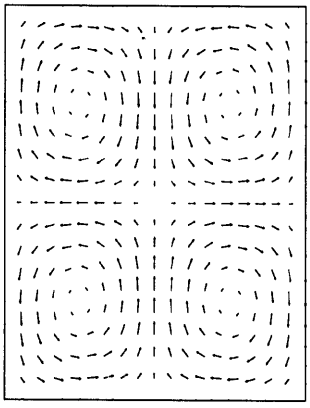

(t)

Figure 2(t). Desired flow at $t = \frac{10}{12}$

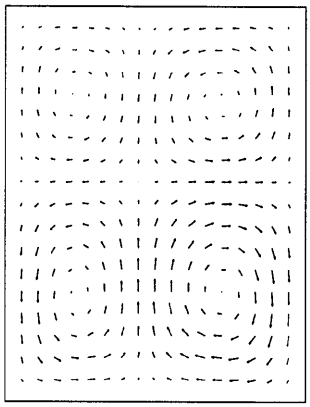

(u)

Figure 2(u). Controlled flow at $t = \frac{11}{12}$

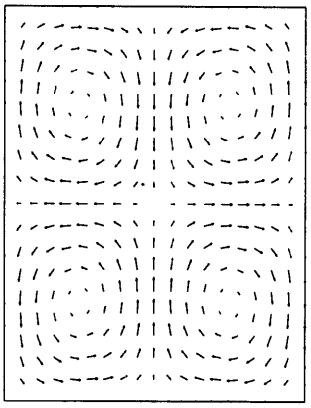

(v)

Figure 2(v). Desired flow at $t = \frac{11}{12}$

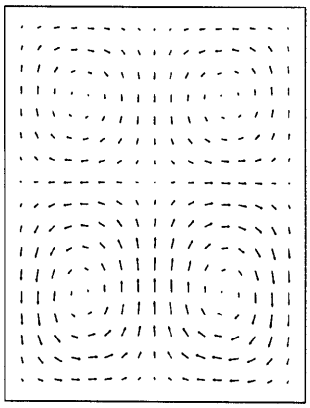

(w)

Figure 2(w). Controlled flow at $t = 1$

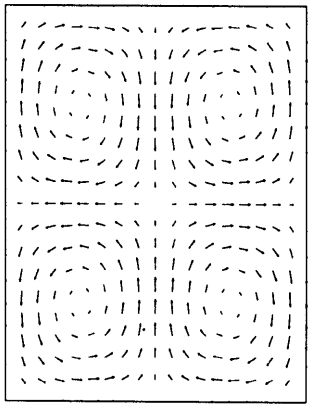

(x)

Figure 2(x). Desired flow at $t = 1$

optimality were given characterizing the controls and optimal states. The computations were carried out using a Newton-like method combined with a mixed finite element method. Although the numerical results for the problems demonstrate the feasibility of the approach, from the computational point of view the underlying optimality system is formidable. Numerical methods to reduce this computational cost using a reduced basis method are currently being developed and will be reported in a forthcoming article.

ACKNOWLEDGEMENTS

This work was supported in part by the Air Force Office of Scientific Research under grants AFOSR F49620-95-1-0437 and AFOSR F49620-95-1-0447.

REFERENCES

1. K. Ito and S. S. Ravindran, 'Optimal control of thermally coupled Navier–Stokes equations', *Proc. 34th Conf. on Decision and Control*, New Orleans, LA, 1995, IEEE, New York, 1995, pp. 461–466.
2. R. Temam, *Navier–Stokes Equations*, *Theory and Numerical Methods*, North-Holland, Amsterdam, 1979.
3. F. Abergel and R. Temam, 'On some control problems in fluid mechanics', *Theor. Comput. Fluid Dyn.*, **1**, 303–325 (1990).
4. H. O. Fattorini and S. S. Sritharan, 'Existence of optimal controls for viscous flow problems', *Proc. R. Soc. Lond. A*, **439**, 81– 102 (1992).
5. M. Gunzburger, L. Hou and T. Svobodny, 'Analysis and finite element approximation of optimal control problems for the stationary Navier–Stokes equations with Dirichlet controls', *Modél. Math. Anal. Numér.*, **25**, 711–748 (1991).
6. S. Sritharan, 'Dynamic programming of the Navier–Stokes equations', *Syst. Control Lett.*, **16**, 299–307 (1991).
7. V. Girault and P.-A. Raviart, *Finite Element Methods for Navier– Stokes Equations*, Springer, Berlin, 1986.
8. M. Gunzburger, *Finite Element Methods for Viscous Incompressible Flow: A Guide to Theory*, *Practice and Algorithm*, Academic, Boston, MA, 1989.
9. R. Glowinski, *Numerical Methods for Nonlinear Problems*, Springer, New York, 1984.

